

Estimating Poverty Using Aerial Images: South African Application

Vongani H. Maluleke^{1,2,*}, Sebnem Er¹, Quentin R. Williams²

¹*PD Hahn Building (South Entrance) Level 5, Upper Campus, Statistical Sciences Department, University of Cape Town, 7700, Cape Town, South Africa*

²*Meraka, CSIR, Meiring Naude Road, 0001, Pretoria, South Africa*

Abstract—Policy makers and the government rely heavily on survey data when making policy-related decisions. Survey data is labour intensive, costly and time consuming, hence it cannot be frequently or extensively collected. The main aim of this research is to demonstrate how deep learning in computer vision coupled with statistical regression modelling can be used to estimate poverty on aerial images supplemented with national household survey data. This is executed in two phases; aerial classification and detection phase and poverty modelling phase. The poverty measure estimated in this paper is the Sen-Shorrocks-Thon index (SST). The models in phase one performed relatively well with the classification model having an accuracy rate of 90.85% and a log loss of 0.5783 while the instance segmentation model has a log-loss of 0.839. The ridge model in phase two also performed well with an R^2 of 0.708, a root mean square error (RMSE) of 0.081, and a strong positive correlation between the estimated SST and actual SST of 0.838 which indicates the strong ability of the model to estimate the SST from the geo-type and dwelling type of an area.

Keywords— Poverty, Computer vision, statistical regression modelling, Aerial Image(s).

I. INTRODUCTION

Poverty is a complex, multi-dimensional phenomenon that constitutes of multiple deprivation aspects [1]. It requires extensive research to comprehend the severity and impact it has in a community. The complexity of poverty is derived from the many factors that it is influenced by, in which the effect of some factors is still unknown.

The National Development Plan (NDP) has been compiled by the South African government to combat poverty and reduce inequality in South Africa by 2030 [2]. Survey data is the main information source to monitor the development and growth of the country to meet the set NDP targets. However, due to limited resources, the collection of survey data is not always conducted frequently nor extensively to a level where the data satisfactory reflects the true livelihood of individuals and household in South Africa.

Currently the South African government is using poverty lines to set and monitor poverty alleviation targets. Poverty line is an index used to divide the population into two groups based on a socio-economic measure such as welfare

[3]. Households or individuals that fall above the poverty line are classified as not poor, while those that fall below the poverty line are classified poor.

There has been a growing interest in the usage of aerial images supplemented with publicly available data to monitor, assess and measure socio-economic indicators, especially with the recent advancements in computer vision. This has also ignited researches in the use of deep learning to address socio-economic related problems.

Some researchers have successfully introduced an approach of using night-time light intensities as a proxy to estimate and map poverty at a country and continental level [4]. They trained a fully convolutional neural network (CNN) to estimate night-time light intensity from day-time aerial images and simultaneously trained another model that captures the effect of the features on the aerial images to estimate poverty. They obtained that day-time aerial images can be utilised to make relatively accurate spatial socio-economic status estimations across Nigeria, Uganda, Malawi, and Tanzania [4].

Recently, [5] further investigated the use of aerial images to estimate poverty and they found that built-up area and roof type have a strong correlation with welfare. They used a deep learning CNN to detect and classify the built-up area and roof type. This paper will demonstrate the use of deep learning in computer vision coupled with statistical regression modelling to estimate poverty in South Africa using aerial images supplemented with longitudinal survey data, with the purpose of developing a tool that will assist the government to combat poverty.

In this paper, the poverty rate is estimated from aerial images by training a deep learning convolutional neural network to detect dwelling types (brick house, traditional house, and informal settlement) and classify geo-types (urban, farm, and rural) from aerial images. This is then followed by training a statistical regression model to estimate the poverty rate, Sen-Shorrocks-Thon index (SST), from the detected dwelling types and geo-types in the aerial images.

II. BACKGROUND

This section will give a foundational understanding of the measures and techniques that will be used to estimate poverty.

A. Poverty Measures

Poverty measures are guiding tools of how poverty is monitored in a country. This is because policy makers construct poverty reduction policies based on how poverty is defined and measured. For instance, in South Africa the government structures policies that will result in more individuals and households living above the poverty line. They further use it to assess the progress they've made by implementing a certain policy.

South Africa has three national poverty lines that the government uses to monitor and measure poverty [6]. The poverty line that is used in this paper is called the Food Poverty Line (FPL), which is the rand value below which individuals or households cannot afford purchasing adequate food to obtain minimum per capita per day energy required for adequate health [6]. These poverty lines were introduced by Statistics South Africa with the intension of enabling the country to measure and monitor poverty on a money-metric or expenditure-based dimension [6].

The poverty line is an imperfect construct that makes the crude assumption of defining poverty by using some minimum level in which people continue to survive below it. However, when making analysis, an index ought to be used to further build understanding of the nature of poverty as argued by [3].

There are many different poverty measures that one can use. The most commonly used measures are namely head count index, denoted as P_0 , and poverty gap index, denoted as P^P_1 [7]. Headcount index represent the incidence of poverty as it measures the proportion of households or individuals who fall below the poverty line. Poverty gap index represents the depth of poverty as it measures the extent of which households and individuals lie below the poverty line [7].

These poverty measures are popularly used because they are easy to compute and understand [7]. However, they only capture one aspect of poverty, which can result in misleading output and hence skewed conclusions. For a robust view of poverty, composite poverty measures are highly recommended [8].

Sen [9] proposed a composite poverty measure called the Sen index, denoted as P_S . This measure considers the population size of the poor, welfare (income or expenditure) shortfall relative to the poverty line and the degree of inequality [9]. The Sen index is defined as:

$$P_S = P_0(P^P_1 + (1-P^P_1)G^P) \quad (1)$$

where P_0 , P^P_1 , G^P is the headcount index, poor population poverty gap and poor population Gini coefficient of the poverty gap ratio. The Gini coefficient is a measure of inequality for a given distribution based on the Lorenz curve [7].

Shorrocks [14] later proposed a modified version of the Sen index which was then later modified by Thon to become the Sen-Shorrocks-Thon (SST) index, denoted as P_{SST} , and defined as:

$$P_{SST} = P_0 P^P_1 (1 + \hat{G}^P) \quad (1)$$

SST index takes into account the depth, incidence and inequality of poverty [7]. It is a more appealing version of the Sen index because the decomposing SST allows for analysis of source of changes in poverty overtime [7]. This decomposition enables us to determine the change in the number of poor people, the change in the level of poor people being poor and the change in the inequality among poor people [7]. In this paper, the SST index is used as the poverty measure and is computed using the survey data.

B. Convolutional Neural Networks

Convolutional neural networks (CNN) is a specialised kind of neural network that uses a mathematical operation called convolution, denoted by $*$, in at least one layer in replacement of the normal neural network matrix multiplication [10]. The convolution operation is defined as:

$$S(i, j) = (I * F)(i, j) = \sum_m \sum_n I(i + m, j + n) * F(m, n) \quad (3)$$

where $I()$ is the input signal and $F()$ is the filter.

A standard CNN contains three types of layers, namely; convolutional, pooling and fully connected layers, where two broad processes happen across the entire network [10]. Collectively the convolutional and pooling layers perform feature extraction, where an image input is passed through the first layers of the network to extract low-level features (edges and corners) and then the last layers extract high-level features (texture and objects) [11].

The convolutional layer is the core layer in CNN, which involves simultaneously performing several convolutions to produce a set of linear activations defined by:

$$a_l = W_l * x + b_l \quad (4)$$

Where W_l is the weights of the l -th convolutional layer filter used to perform convolution ($*$) on the image or feature map, denoted x , offset by the l -th layer bias (b_l). The linear activation is then passed through a non-linear function ($f_l(a_l)$). Rectified linear unit (ReLU) is popularly used as the non-linear function in classification tasks because it has low computational complexity and it has an ability to maintain the scale of output values [10].

In the pooling layer, a pooling function is applied to the convolutional layer output. This layer is used to reduce the size of the image to speed the computation of the model. Max pooling and average pooling are popularly used in CNN to down sample the image spatially.

The final layer of a standard CNN is a fully connected layer that uses the final output of the feature extraction process, called a feature map, to perform classification. This is executed by matrix multiplication of the neurons with an offset of the bias to output a K dimensional vector using soft-max. Where K is the number of classes and each

element in the output is the probability of the image input belonging to the k -th class.

C. Mask R-CNN

Mask R-CNN is a type of instance segmentation CNN model that is used to perform instance object detection by identifying the outlines of objects at pixel level [12]. It is

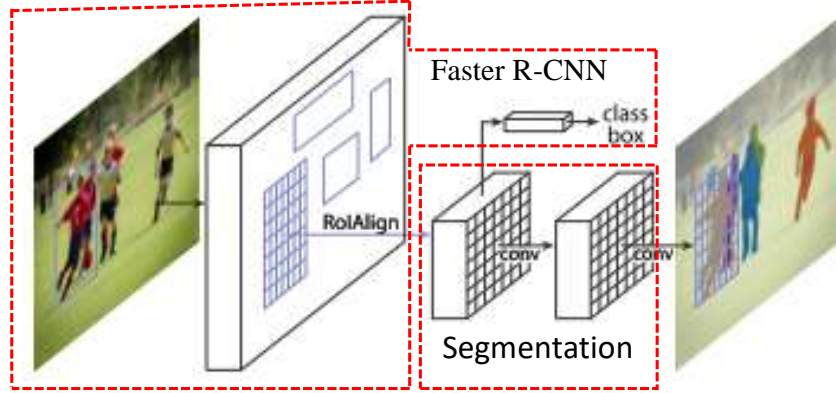


Fig. 1. Mask R-CNN architecture. Extension of Faster R-CNN with a segmentation branch and RoIAlign for accurate mapping between original image and proposal [12].

Firstly, an image is passed through a CNN backbone model where low-level and high-level features are extracted. This backbone network model outputs a feature map which becomes the input for proceeding stages. The feature map from the backbone model is then passed through a region proposal network (RPN) where the network uses a sliding window to scan the feature map with the purpose of finding regions that are likely to contain an object called proposals (regions of interest). These regions that are scanned to find proposals are called anchors, which are overlapping boxes of different aspect ratios and sizes distributed all over the feature map.

Once the proposals have been generated by the RPN, each proposal is passed into a Faster R-CNN to perform classification and localisation to output a class label and a four-valued bounding box tuple (x, y, w, h) , respectively. Simultaneously, a Fully Convolutional Network (FCN) is applied to each proposal to predict the mask of the detected object instance. This mask is a binary encoding of the spatial layout of the object, where pixels that belong to the object are encoded with the value one and zero otherwise [12].

RoIAlign was introduced in Mask R-CNN to avoid misalignment between the original image and feature map caused by quantisation in RoIPool, which is observed in Faster R-CNN when a feature map is resized into a fixed size [12]. RoIAlign allows for accurate mapping of the proposals from the original image onto a feature map.

$$\mathcal{L} = \mathcal{L}_{cls} + \mathcal{L}_{bbox} + \mathcal{L}_{mask}$$

The loss function of the Mask R-CNN is defined on each proposal during training as the combination of the log loss of classification (\mathcal{L}_{cls}), localisation (\mathcal{L}_{bbox}) and segmentation mask (\mathcal{L}_{mask}) and is given by:

where \mathcal{L}_{cls} is multi-class cross entropy for the class

essentially a combination of object detection and semantic segmentation, where an additional branch in Faster R-CNN is added to generate a segmentation output as seen in Fig. 1. According to [12], it currently outperforms all existing single-model entries on every task. Furthermore, it is easy to train and to generalise to other tasks [12].

labels, \mathcal{L}_{bbox} is the smoothed $L1$ loss for the bounding box and \mathcal{L}_{mask} is the average cross entropy loss for the masks. A model that performs well has a log loss that is close to zero.

A. Statistical Regression Modelling: Ridge Regression

Statistical regression is a tool used for the identification and characterisation of the functional relationships between the dependent variable and p independent variables [13]. In this paper, the dependent variable is the SST and the independent variables are the number of detected dwelling types found within each geo-type.

Ridge regression is an extension of multiple linear regression that is used for analysing multiple regression data suffering multicollinearity [13]. Ridge regression was first introduced by [14] to improve the instability of the ordinary least squares (OLS) estimators and has since been popularly used to get improved prediction results.

Ridge regression is also known as a shrinkage method that shrinks parameters zero by imposing an $L2$ penalty ($\sum_{j=1}^p \beta_j^2$) on their size [13]. It assigns low weights to variables that explain less variance [13]. Parameters in ridge regression are estimated by minimising the penalised residual sum of squares (RSS) defined as:

$$\hat{\beta}^{ridge} = \underset{\beta}{\operatorname{argmin}} \sum_{i=1}^n (y_i - \beta_0 - \sum_j \beta_j x_{ij})^2 = \underset{\beta}{\operatorname{argmin}} \operatorname{RSS}(\beta) \quad (5)$$

$$\text{Subject to: } \sum_j \beta_j^2 \leq t \quad (6)$$

which can also be represented in Lagrangian form as:

$$\mathcal{L}(\beta, \lambda) = \underset{\beta}{\operatorname{argmin}} \sum_{i=1}^n (y_i - \beta_0 - \sum_j \beta_j x_{ij})^2 + \lambda \sum_j \beta_j^2 \quad (7)$$

A. National Geo-Spatial Information (NGI) Aerial Images

The aerial images were provided by the National Geo-Spatial Information (NGI) and are concurrent with the NIDS data. The images provided have a resolution of 34000x34000 and for classifying and detecting dwelling types and geo-types, these images were cropped into

300x300 resolution images. This was implemented by overlaying a grid with 300x300 sized cells as shown in Fig. 3. A python package called labelme.py was used to manually label the aerial images [17]. For accurate and consistent labelling, NIDS data was used to assist with the labelling.



Fig. 3. a) Original image b) Grid Overlaid image, with 2931CC topological code.

I. METHODOLOGY

Estimating poverty is executed in two phases namely the aerial classification and detection phase and the poverty modelling phase.

A. Phase1: Aerial classification and detection

This phase firstly involves classifying three classes of geo-types (urban, rural and farm) using a CNN model with three convolutional layers, each layer followed by a max-

pooling layer. This classification model architecture is depicted in Fig. 4, where an image is passed through the convolutional layers and max-pooling layers to perform feature extraction and then through a fully connected layer which uses a soft-max to output the probability of the image belonging to the three broad geo-type classes namely; urban, rural, and farm.

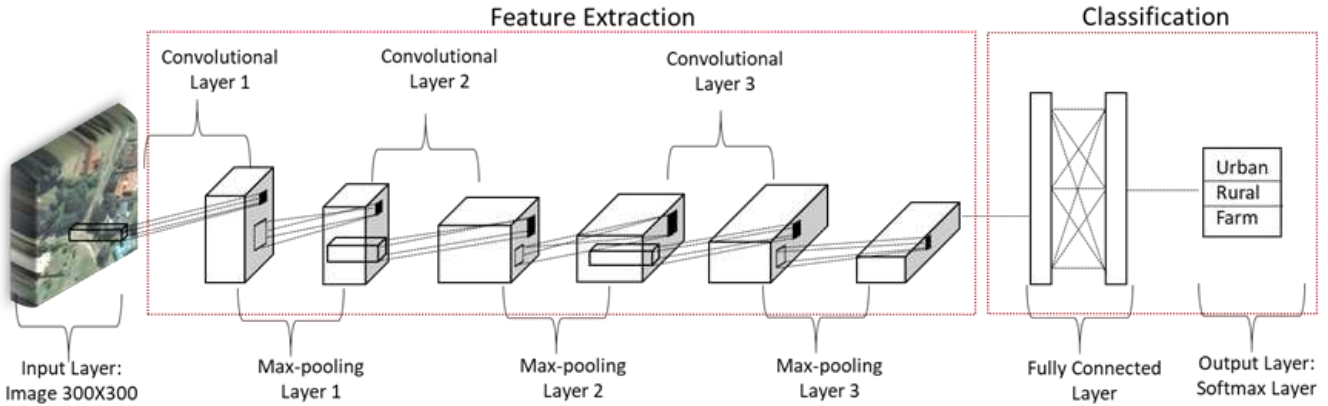


Fig. 4. Convolutional Neural Networks (CNN) model architecture used to perform geo-type (urban, rural, and farm) classification on aerial images.

Next, a Mask R-CNN model is trained on the same labelled images to detect three broad classes of dwelling types namely; brick house, traditional house, and informal settlement. Fig. 5 shows the detection model architecture, where the training data images are passed through a ResNet101 CNN, which is the backbone CNN of this model, to perform feature extraction and output a feature

map that is used to generate proposals by the RPN. For each proposal made, three tasks are simultaneously performed to output the class label, bounding box coordinates and the mask. Different mask colours are used to show different object instances detected as seen in Fig. 5 output.

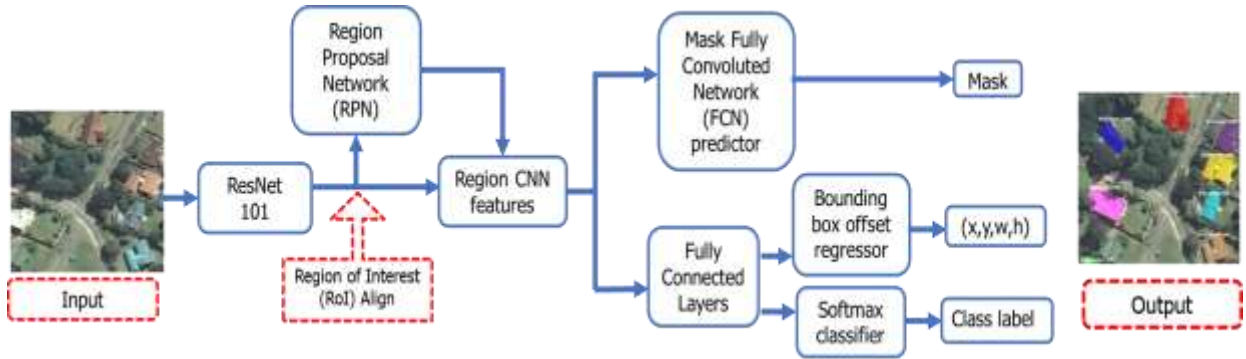


Fig. 5. Mask Region-based Convolutional Neural Networks (Mask R-CNN) model architecture used to perform dwelling-type (brick house, traditional house, and informal settlement) detection on aerial images.

A. Phase2: Poverty Modelling

In this phase, the NIDS data was used to compute the SST and the corresponding vectorised cross Table of the geo-type and dwelling type for each topological code. This was then used to train a ridge regression model where the computed SST is the dependent variable and the items in the vectorised cross table are independent variables.

B. Final Model

The architecture of the final poverty estimation model constitutes of phase one and phase two trained models, as

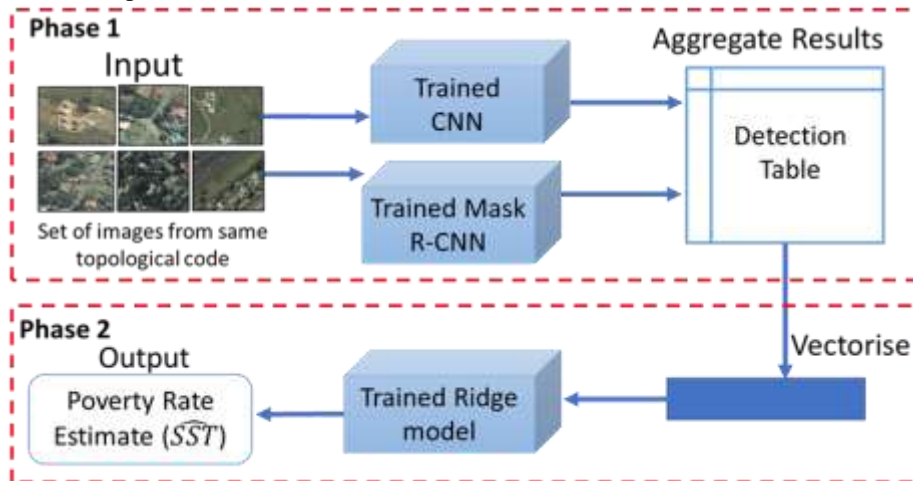


Fig. 6. Architecture of the final poverty estimation model.

I. RESULTS

A. Phase 1 results

The models in phase one perform significantly well, Table II and Table III summaries phase one result. The geo-type classification model classifying images into three geo-type classes has a high accuracy rate of 0.9085 and a relatively low log-loss of 0.5783. The accuracy rate indicates that the classification model has correctly classified 90.85% of the images. The log-loss captures the uncertainty of the classifications made based on the amount of divergence between the predicted probabilities of class from the actual class labels. The low log-loss of 0.5783 indicates that there is minimal divergence between predicted classification probabilities made by the geo-type classification model and the actual class labels.

The dwelling type detection model has a log-loss of 0.839 which is the sum of the class label loss, bounding box loss

shown in Fig. 6. To estimate poverty and create a poverty distribution map, a set aerial images for a certain location (topological code, district, or province) is used as input and classification of geo-type and detection of dwelling type is performed individually on each image. The classified geo-types and detected dwelling types are then aggregated and used as input in phase 2 to estimate the poverty rate, SST, using a trained ridge regression.

and mask loss. From Table III, the class label loss is the lowest loss with a loss of 0.219, followed by the bounding box and mask loss with a loss of 0.220 and 0.401, respectively. These three losses each indicate that there is minimal divergence between the predicted probabilities and actual values of the class labels, bounding box tuple and binary mask, respectively.

TABLE II. PERFORMANCE RESULTS OF THE GEO-TYPE CLASSIFICATION MODEL

Metric	Geo-type Classification Model
Accuracy rate	0.9085
Log loss	0.5783

TABLE III. PERFORMANCE RESULTS OF THE DWELLING-TYPE DETECTION MODEL

Metric	Dwelling Type Detection Model
Log loss	0.839
Class label loss	0.219
Bounding box loss	0.220
Mask loss	0.401

B. Phase 2 results

The performance of the ridge regression model has been summarised in Table IV. The optimal tuning parameter, $\lambda = 0.032$, was obtained by using ten-fold cross-validation. This optimal tuning parameter corresponds to the minimum cross-validation error of the model. The resultant ridge regression model with the optimal λ produces an R^2 of 0.708 which means that the geo-type dwelling type variables explains 70.80% of the variation in the SST poverty rate. Furthermore, the root mean square error (RMSE) of the ridge model is 0.081 which indicates that the ridge model fits the data well.

There is a positive strong correlation (r) of 0.838 between the estimated SST and the observed SST, indicating the strong ability of the model to estimate SST from the classification of geo-types and detection of dwelling types from aerial images. This can also be seen in Fig. 7, where

the points lie relatively close to the red 45° line. Observations that lie on the red line have been accurately estimated. From Fig. 7, it is observed that the model tends to over-estimate (data points lie above the red line) the SST value when there is low poverty (low SST) and under-estimate estimate (data points lie below the red line) when there is high poverty (high SST).

TABLE IV. PERFORMANCE RESULTS OF THE RIDGE REGRESSION MODEL.

Metric	Ridge Regression Model ($\lambda = 0.032$)
R^2	0.708
r	0.219
RMSE	0.220

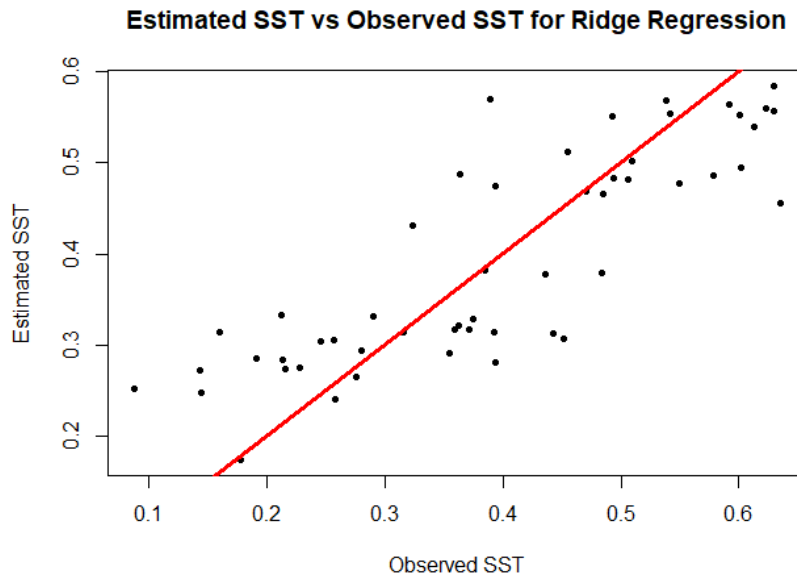


Fig. 7. Estimated SST vs Observed SST for NIDS wave 4.

I. CONCLUSION

This paper introduced an approach to estimate poverty from aerial images by using deep learning computer vision models coupled with a statistical regression model. This approach involves detecting the geo-types and dwelling-types from aerial images and then aggregating the results to estimate the poverty index, SST, which is a composite poverty measure that captures a robust view of poverty. The application of this approach was demonstrated by using aerial images of KwaZulu-Natal, South Africa. This approach displays great potential in becoming a tool that the government can use to efficiently measure, monitor and analyse the poverty rate as they implement policies targeted to alleviate poverty. Considering other features that can be detected or identified using computer vision such as mines, police stations, hospitals, water sources, road type, etc. can be used to improve the model to estimate poverty.

II. ACKNOWLEDGEMENTS

We would like to acknowledge DataFirst and National Geo-spatial information (NGI) for the provision of survey data and aerial images respectively and for the data support from Lynn WoolFrey and Alex Montgomery.

REFERENCES

- [1] D. Narayan, R. Patel, K. Schafft, A. Rademacher, and S. Koch-Schulte. *Voices of the poor: can anyone hear us?*. New York: Oxford University Press. 2000. [Online]. Available: <http://documents.worldbank.org/curated/en/131441468779067441/Voices-of-the-poor-can-anyone-hear-us>.
- [2] National Planning Commission. *Our future-make it works*. 2011.
- [3] H. Bhorat, M. Leibbrandt, M. Maziya, S. van der Berg, and I. Woolard. *Fighting Poverty-Labour Markets and Inequality in South Africa*. UCT Press. 2001
- [4] M. Xie, N. Jean, M. Burke, D. Lobell, and S. Ermon. "Transfer Learning from Deep Features for Remote Sensing and Poverty Mapping." 2015. CoRR abs/1510.00098. <http://arxiv.org/abs/1510.00098>.
- [5] R. Engstrom, S.H. Jonathan, and D.L. Newhouse. "Poverty from Space: Using High Resolution Satellite Imagery for Estimating Economic Well-being". Washington, D.C: World Bank Group. 2017. [Online]. Available:

- <http://documents.worldbank.org/curated/en/610771513691888412/Poverty-from-space-using-high-resolution-satellite-imagery-for-estimating-economic-well-being>.
- [6] Statistics South Africa. *National Poverty Lines*. Technical report, Pretoria: Statistics South Africa. 2018.
- [7] J. Haughton, and R. Khandker. *Handbook on Poverty and Inequality*. Washington, DC: The World Bank. 2009.
- [8] P. Govender, N. Kambaran, N. Patchett, A. Ruddle, G. Torr, and N. Zyl. "Poverty and Inequality in South Africa and the world." doi:10.4314/saaj.v7i1.24511. 2007.
- [9] A. Sen. "Poverty: An Ordinal Approach to Measurement." *Econometrica*, 219-231. 1976.
- [10] I. Goodfellow, Y. Bengio, and A. Courville. *Deep Learning*. MIT Press. 2016. [Online]. Available: <http://www.deeplearningbook.org>.
- [11] M.D. Zeiler, and R. Fergus. "Visualizing and Understanding Convolutional Networks." *CoRR abs/1311.2901*. 2013. [Online]. Available: <http://arxiv.org/abs/1311.2901>.
- [12] K. He, G. Georgia, P. Dollar, and R. Girshick "Mask R-CNN." *CoRR abs/1703.06870*. 2017. [Online]. Available: <http://arxiv.org/abs/1703.06870>.
- [13] G. James, D. Witten, T. Hastie, and R. Tibshirani. *An Introduction to Statistical Learning with Applications in R*. Springer New York Heidelberg Dordrecht. 2013.
- [14] A.E. Hoerl, and R.W. Kennard. "Ridge Regression: Biased Estimation for Problems Nonorthogonal." *Technometrics* 55-67.
- [15] Southern Africa Labour and Development Research Unit. 2016. "National Income Dynamics Study 2014 - 2015, Wave 4 [dataset]. Version 1.1." Cape Town: Southern Africa Labour and Development Research Unit [producer]. (Cape Town: DataFirst [distributor], 2016. Pretoria: Department of Planning Monitoring and Evaluation [commissioner], 2014). 1970.
- [16] University Michigan State. n.d. *South Africa 1:50,000*. [Online]. Available: https://lib.msu.edu/branches/map/findingaids/SouthAfrica50k_KZN/.
- [17] Tzutalin. *labelimg*. 2015.
- [18] V. Kshirsagar, J. Wieczorek, S. Ramanathan, and R. Wells. "Household poverty classification in data-scarce environments: a machine learning approach." 2017. arXiv preprint arXiv:1711.06813.